Optical and electrical properties of vanadium oxides synthesized from alkoxides

Jacques Livage *

Chimie de la Matière Condensée, UMR CNRS 7574, Université Pierre et Marie Curie, 4 place Jussieu, 75252 Paris, France

Contents

Abstract

Vanadium oxides have been synthesized via the hydrolysis and condensation of vanadium alkoxides $VO(OR)_3$. Different materials are actually obtained depending on the hydrolysis ratio $h = H_2O/V$. Spin-coated alkoxides lead to vanadium dioxide. These thermochromic VO_2 thin films exhibit a metal-insulating transition. They are transparent at room tempera-

* Tel.: + 33-1-44273365; fax: + 33-1-44274769.

E-mail address: livage@ccr.jussieu.fr (J. Livage)

ture and IR reflecting above 70°C. The transition temperature can be easily modified by doping with other metal cations. Amorphous oxo-polymers are formed via the partial hydrolysis of vanadium alkoxides. They give optically transparent thin films that could be used in electrochromic display devices. The hydrolysis of vanadium alkoxide in the presence of an excess of water leads to ribbon-like particles of hydrated oxide $V_2O_5 \cdot nH_2O$. Mesophases are observed in vanadium oxide gels and sols that exhibit a nematic liquid crystal behavior. They can even be oriented by applying a magnetic field. Anisotropic thick films can be deposited from these gels. They exhibit a strong preferred orientation. Mixed proton and electron conduction is observed in these gels that can be used as reversible cathodes for lithium batteries. © 1999 Elsevier Science S.A. All rights reserved.

1. Introduction

Sol-gel chemistry has been widely developed during the past decade for the synthesis of glasses and ceramics [1]. It is based on the inorganic polymerization of alkoxide precursors. Polymerization is initiated via hydrolysis in order to obtain reactive M–OH groups. Condensation then occurs leading to the formation of an oxide network. Condensed species are progressively formed from the solution leading to oligomers, oxo-polymers, colloids and gels [2]. One of the main advantages of the sol-gel route is to allow the powderless processing of glasses and ceramics [3]. Thin films for instance can be deposited directly from the solution by such techniques as spin or dip-coating.

This paper describes the properties of vanadium oxides synthesized from vanadium alkoxides $VO(OR)_3$. They exhibit both electronic and ionic properties and appear to be good candidates for the production of smart thin films. Electronic properties arise from the mixed valence behavior of vanadium. Electron hopping occurs between metal ions in different oxidation states (V^{5+}–V^{4+}) giving rise to semiconducting properties and specific optical absorption. Ionic properties arise from the acid dissociation of V–OH groups at the V_2O_5–H_2O interface [4].

The molecular design of alkoxide precursors provides a chemical control over condensation reactions allowing the synthesis of tailor made materials. Different compounds can be obtained depending on the hydrolysis ratio $h = H_2O/VO(OR)_3$ (R = alkyl group). Oriented thick coatings or optically transparent amorphous thin films can be obtained depending on hydrolysis conditions. These vanadium oxide films appear to be a good candidate for the realization of micro-batteries, electrochromic display devices or optical switches.

2. Thermochromic properties of VO_2 thin films

2.1. Synthesis of VO_2 thin films

Vanadium oxide thin films have been deposited from vanadium alkoxide solu-

tions [5]. Vanadium alkoxides $VO(OR)_3$ ($R = Pr^i$, Am^t) are synthesized via the reaction of ammonium vanadate with the corresponding alcohol as follows:

$$NH_4VO_3 + 3ROH \Rightarrow VO(OR)_3 + 2H_2O + NH_3$$

The reaction is carried out in cyclohexane and the mixture is heated under reflux. Water is removed via azeotropic distillation. The vanadium alkoxide is purified by distillation under reduced pressure and then dissolved in its parent alcohol.

The chemical reactivity of vanadium alkoxides toward hydrolysis mainly depends on the steric hindrance of the alkoxy group [3]. $VO(OPr^i)_3$ is then more reactive than $VO(OAm^t)_3$. $VO(OPr^i)_3$ being commercially available, most experiments are performed with this precursor. However, $VO(OPr^i)_3$/Pr^iOH solutions are rapidly hydrolyzed and have to be stabilized by adding a complexing reagent such as acetyl acetone or acetic acid [6]. $VO(OAm^t)_3$ is less reactive but it is too viscous and defect free films have not been obtained from $VO(OAm^t)_3$/Am^tOH solutions. The best results have been obtained with a 0.7 M solution of $VO(OAm^t)_3$ in Pr^iOH. Transesterification reactions then occur giving rise to $VO(OAm^t)_{3-x}(OPr^i)_x$ species ($0 \leq x \leq 3$). ^{51}V NMR spectra of such a solution shows that it contains a mixture of the four species in the following molar ratio $x = 0$ (0.5%), $x = 1$ (11%), $x = 2$ (39%) and $x = 3$ (49.5%) (Fig. 1).

The akoxide solution is spin-coated onto a silica substrate and rapidly dried around 80°C with an IR heater so that hydrolysis remains negligible. A very thin layer, about 600 nm in thickness, is obtained and three successive coatings have been deposited in order to get thicker films (≈ 0.2 μm).

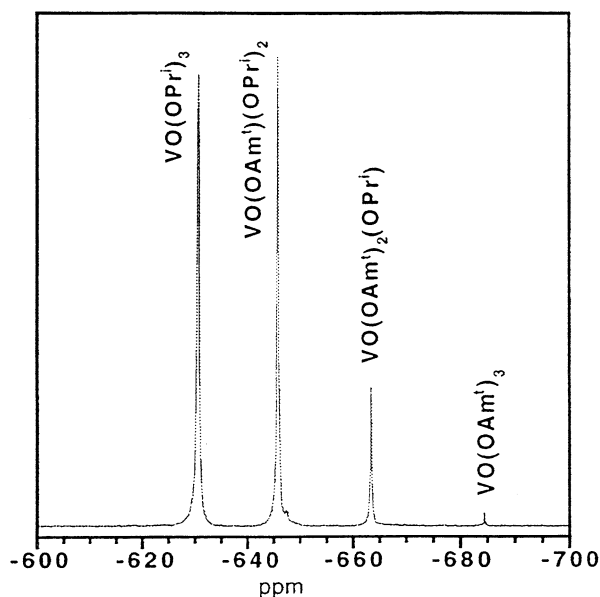Fig. 1. ^{51}V NMR spectrum of a 0.7 M solution of $VO(OAm^t)_3$ in Pr^iOH.

As deposited alkoxide films appear to be amorphous by X-ray diffraction. They have to be heat treated in a reducing atmosphere in order to remove all organics and allow the formation of crystalline VO_2. Heating in air would lead to fully oxidized V_2O_5. Many vanadium oxides can be obtained in the V–O phase diagram, so that experimental conditions have to be carefully controlled. Heating the film for 2 h at 500°C under a reducing gas flow (Ar–H_2 5%) actually leads to optically transparent and homogeneous films corresponding to the pure VO_2 phase as checked by X-ray diffraction [5].

2.2. Electrical switching

Electrical resistance measurements were performed in the 20–100°C temperature range using the four-probes method. A typical hysteresis loop is observed. Upon heating, the resistance drops rapidly by about three orders of magnitude above 70°C. Upon cooling, the insulating state is recovered at a lower temperature, around 60°C (Fig. 2(a)).

Electrical switching devices have been made via the deposition gold electrodes at the surface of a VO_2 film [7]. These electrodes are evaporated through a mask so that the geometry of the inter-electrode space can be accurately controlled. An a.c. voltage (50 Hz) is applied to the device and the intensity–current (I–V) curve is recorded onto an oscilloscope (Fig. 2(b)). The film remains in the insulating 'OFF' state below the threshold voltage ($V_{th} \approx 50$ V). However, as the intensity increases, the film is heated via the Joule effect and the vanadium dioxide turns metallic when its temperature becomes larger than $T_c \approx 70$°C. The device remains in the 'ON' state as long as the intensity is larger than the holding current $I_h \approx 0.6$ mA. Below this point, the film switches back to the 'OFF' state. This switching behavior can be observed continuously for several weeks or even months. This points out the high reversibility of such devices based on VO_2 thin films. Bulk materials do not withstand cycling. The structural distortion associated with the insulator-metal transition rapidly breaks single crystals after few cycles only.

2.3. Optical switching in pure and doped VO$_2$ thin films

The optical transmission of VO_2 thin films was measured in the IR ($\lambda = 2.5$ μm) in the temperature range 15–100°C. As for electrical resistance, IR transmittance exhibits a typical hysteresis loop around the transition temperature (Fig. 3). For pure VO_2 films, optical switching occurs around 80°C upon heating and below 60°C upon cooling. In the metallic state, optical transmittance drops by almost two orders of magnitude and becomes smaller than 1%, showing that the reflectivity of VO_2 films in the metallic state is quite high.

The transition temperature T_c of VO_2 can modified by doping. Doped M_xVO_2 (M = W^{6+}, Nb^{5+}, Ti^{4+}, Al^{3+}) thin films can be easily made by dissolving a salt or an alkoxide of the doping element in Pr^{i}OH and mixing this solution with that of the vanadium precursor. Films are then heat treated as previously [8]. The temperature at which switching occurs is significantly smaller, around 40°C upon
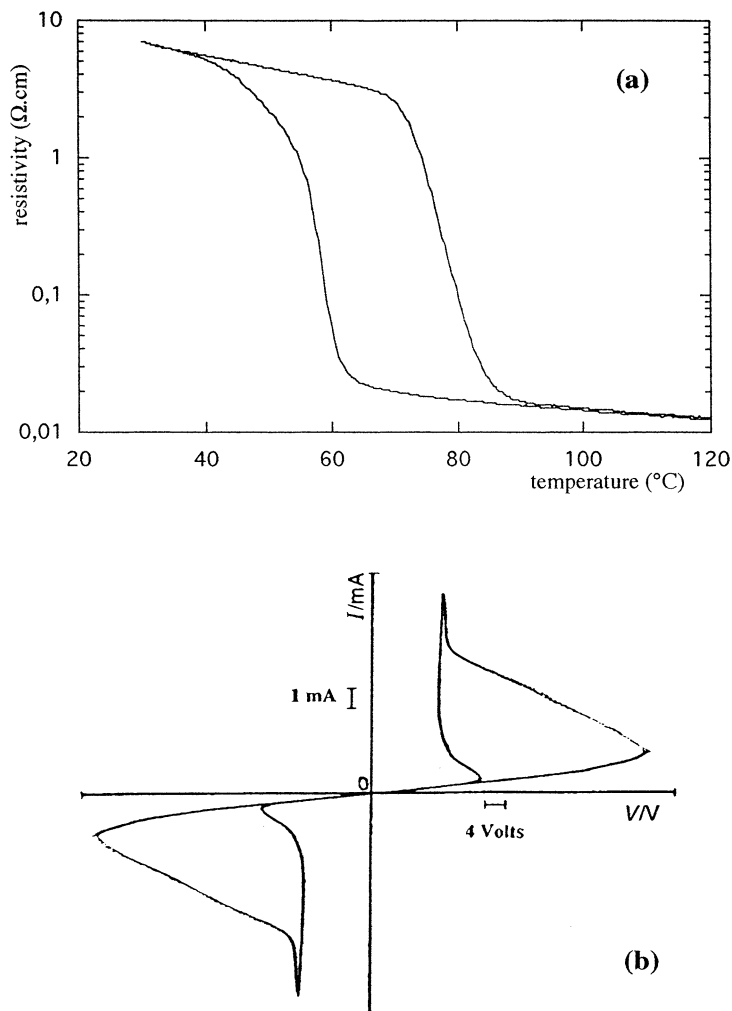
Fig. 2. Metal-insulating transition of VO$_2$ thin films. (a) Electrical resistance as a function of temperature. (b) I–V characteristic of a switching device.

heating, when the film is doped with 2% W^{6+}. Transition close to ambient temperature can even be obtained when the amount of tungsten reaches 5%. The reverse is observed with Al^{3+} doped VO$_2$ films for which the optical switching occurs around 90°C upon heating.

3. Electrochromic properties of amorphous oxo-polymers

Amorphous oxo-polymers are formed when the alkoxide film is left in air for few hours. Hydrolysis occurs spontaneously due to ambient humidity giving rise to

partially hydroxylated $VO(OR)_{3-x}(OH)_x$ species. Non hydrolyzed alkoxy groups prevent the formation of an oxide network and amorphous oxo-polymers rather than vanadium oxides are formed. Some reduction occurs upon drying due to the remaining organic components and mixed valence thin films exhibiting some electronic conductivity arising from an electron hopping between V^{4+} and V^{5+} ions along the V–O–V network ($\sigma_{300} \approx 10^{-3}\ \Omega^{-1}\ cm^{-1}$).

Cyclic voltammetry experiments show that Li^+ ions can be reversibly inserted within these amorphous films (Fig. 4) in the potential range $-1.5, +1$ V (vs. Ag/Ag$^+$). The working electrode is made of a vanadium alkoxide thin film deposited onto a transparent electrode (SnO$_2$:F). The electrolyte was a solution of LiClO$_4$ (1 M) in propylene carbonate. Voltammograms exhibit featureless reduction
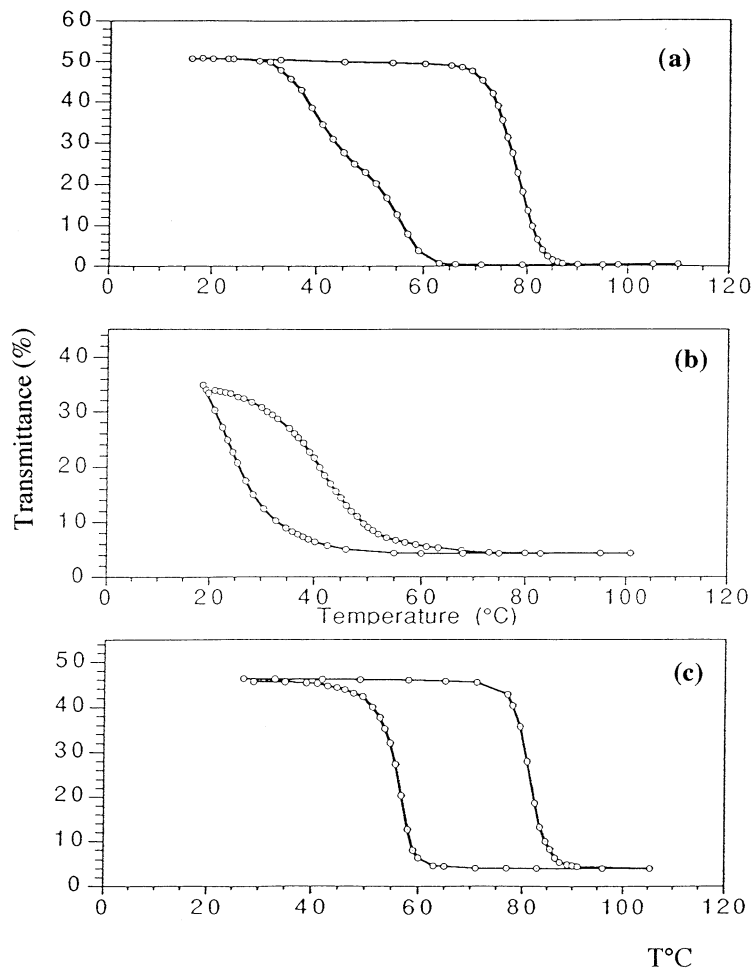

Fig. 3. Optical switching in pure and doped M_xVO_2 thin films ($\lambda = 2.5$ μm). (a) VO$_2$; (b) M = W^{6+}, $x = 0.02$; (c) M = Al^{3+}, $x + 0.02$.
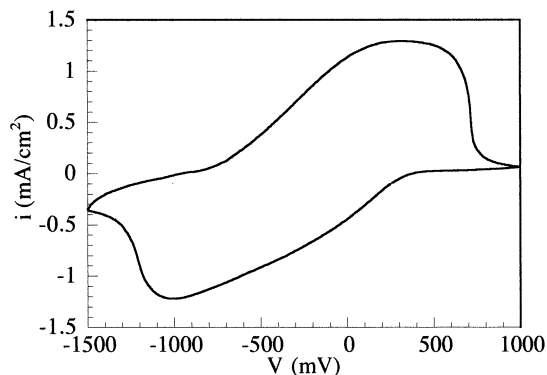
Fig. 4. Cyclic voltammogram of an amorphous vanadium oxo-polymer film.

and oxidation curves typical of an amorphous compound. The charge inserted during the first cycle is smaller than for crystalline V_2O_5. This might be due to the reduction state of the film ($V^{4+}/V^{5+} \approx 10\%$). However, insertion appears to be more reversible and a charge of 40 mC cm^{-2} is still exchanged after 20 cycles.

Optical absorption measurements performed during cyclic voltammetry experiments show that the coloration of amorphous thin films changes progressively during the reduction–oxidation cycle. They turn from yellow to green and blue upon reduction. The process is highly reversible and optical switching occurs within a few seconds when a voltage of $+2$ V is applied [9]. Optically transparent thin films deposited from vanadium alkoxides could therefore be used for the realization of electrochromic devices. However, their absorption in the visible region is quite low and thick films are required to obtain a good optical contrast. Thin films should then be used as counter electrodes in electrochromic devices [10].

As for VO_2, these films can be easily doped by mixing two alkoxides in the precursor solution. Amorphous thin films were then obtained via the deposition of a mixture of $VO(OAm^t)_3$ and $Ti(OPr^i)_4$ (90–10) in Pr^{i}OH. They exhibit improved electrochemical properties. In total 62 mC cm^{-2} are inserted during the first cycle and 56 mC cm^{-2} after 20 cycles [6].

4. Hydrated vanadium oxide gels

### 4.1. Layered structure of $V_2O_5 \cdot nH_2O$ gels

Completely different materials are obtained when a large amount of water ($h \approx 10$) is added to the vanadium alkoxide solution. All alkoxy groups are then fully hydrolyzed and a viscous red gel, $V_2O_5 \cdot nH_2O$, is formed [4].

The formation of such a gel can be described as follows. The full hydrolysis of $VO(OR)_3$ leads to $VO(OH)_3$. In the presence of an excess of water coordination expansion occurs via the addition of two water molecules. A six-fold coordinated

precursor [VO(OH)$_3$(OH$_2$)$_2$] may be formed in which a weakly bonded water molecule lies along the axial direction opposite to the short V=O double bond (Fig. 5(a)). Condensation cannot occur along this direction as there is no V–OH group. Condensation occurs only within the equatorial plane either via olation along H$_2$O–V–OH or oxolation along HO–V–OH. These two directions are not equivalent as olation usually proceeds faster than oxolation. Condensation then leads to a ribbon-like oxide species (Fig. 5(b)). Such ribbons can be clearly seen by electron microscopy. They are about 0.5 μm long, 10 nm wide and 1 nm in thickness [11]. The 1-D Patterson map deduced from X-ray diffraction experiments suggests that the structure of these ribbons is close to that of orthorhombic V$_2$O$_5$ Fig. 6. They are made of two V$_2$O$_5$ sheets facing each other at a distance of 2.8 Å [12].

4.2. Liquid crystal behavior of $V_2O_5 \cdot nH_2O$ gels

In the presence of an excess of water vanadium oxide gels exhibit acid properties due to the acid dissociation of V–OH groups at the oxide/water interface:

$$> V-OH + H_2O \Leftrightarrow > V-O^- + H_3O^+$$
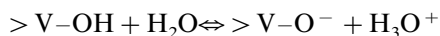
Vanadium oxide gels then behave as 'polyoxovanadic acids' H$_x$V$_2$O$_5 \cdot n$H$_2$O. The pH of the aqueous medium decreases down to pH 2. Protometric titration shows that about 0.3 protons per V$_2$O$_5$ can be ionized ($x \approx 0.3$). Vanadium oxide ribbons then
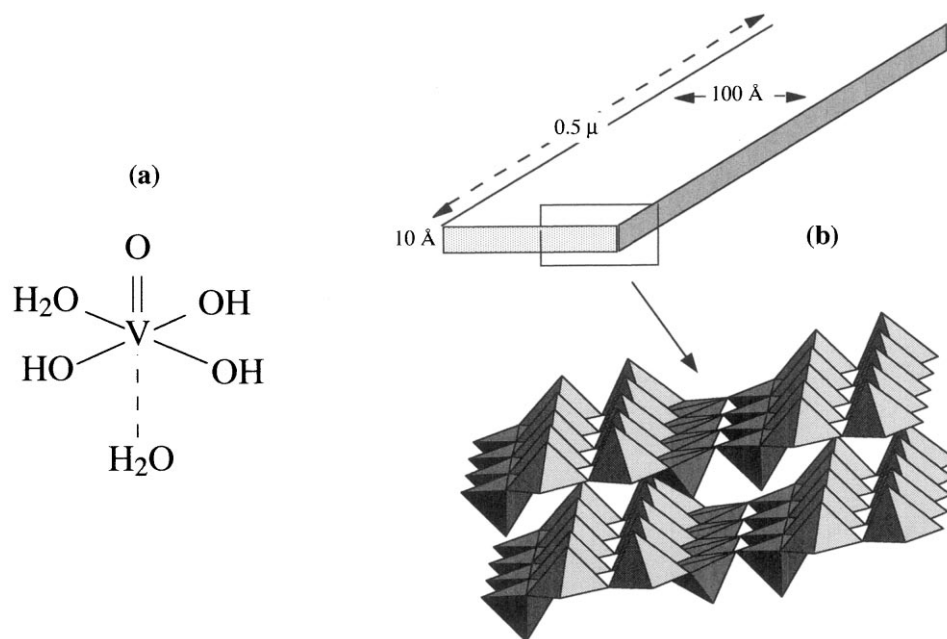

Fig. 5. Formation of V$_2$O$_5 \cdot n$H$_2$O gels: (a) suggested precursor [VO(OH)$_3$(OH$_2$)$_2$]; (b) ribbons structure of the gel, ribbons are made of double chains of [VO$_5$] pyramids as in orthorhombic V$_2$O$_5$.

bear the corresponding negative charge. Electrostatic repulsions prevent the precipitation of oxide particles and are responsible for the stability of the dispersion of vanadium oxide ribbons in aqueous suspensions.

Moreover, the anisotropic shape of V_2O_5 ribbons leads to the formation of mesophases in aqueous vanadium oxide suspensions [13]. This is one of the very few examples of mineral lyotropic liquid crystals [14]. When observed by optical microscopy between crossed polarizers, vanadium oxide sols and gels display optical textures typical of nematic liquid crystals. These textures arise from the formation of topological defect lines called disclinations. The nematic phase displays a reversible sol/gel transition around $n \approx 250$ and different textures can be observed depending on the V_2O_5 concentration. Sols display classical 'Schlieren' textures whereas gels exhibit a 'banded texture' made of regularly spaced dark bands lying perpendicular to the shear flow direction. The dark brushes correspond to the regions where the ribbons are either parallel or perpendicular to the polarizers axis. Such a texture is currently displayed by nematic polymers and points out the similarity of V_2O_5 sols with nematic solutions of semi-rigid polymers. Nematic gels and sols turn isotropic in dilute suspensions ($n > 600$). Dilute nematic sols can be oriented along any direction by applying a magnetic field as low as 0.2 T. This is due to the strong diamagnetic anisotropy of the ribbons and their cooperative behavior in nematic sols. Isolated ribbons cannot be oriented in more diluted isotropic sols [15].

4.3. Intercalation properties of $V_2O_5 \cdot nH_2O$ gels

The nematic ordering can be preserved upon drying. When deposited onto a flat substrate and dried at room temperature (r.t.) vanadium pentoxide gels give rise to xerogel layers ($n \approx 1.8$) that exhibit some preferred orientation [16]. X-ray diffraction of these xerogels display the *00l* peaks typical of a turbostratic stacking of the V_2O_5 ribbons along a direction perpendicular to the substrate (Fig. 6). Water molecules are intercalated between the ribbons and the basal distance increases by steps of about 2.8 Å when the amount of water increases ($d = 8.7$ Å for $n = 0.5$ and $d = 11.5$ Å for $n = 1.8$) [17].

A wide range of ionic or molecular species can be intercalated within the layered structure of $V_2O_5 \cdot nH_2O$ xerogels. Intercalation reactions are much easier than with crystalline compounds. They occur within a few minutes at r.t. Intercalation is mainly due to ion exchange with the acid protons of the gel, but molecular exchange or vanadium reduction may also be involved [4]. The intercalation of organic molecules within the layered structure of $V_2O_5 \cdot nH_2O$ gels leads to a whole range of hybrid materials. The intercalation of organic monomers such as aniline, pyrrole or thiophene, followed by their in situ polymerization leads to a new class of nanocomposites in which a variety of electronically conducting organic polymers are inserted between the 2D structure of the oxide layers [18–20]. Polymers such as polyethylene oxide (PEO) or polyethylene glycol (PEG) have been intercalated within the layered structure of $V_2O_5 \cdot nH_2O$ gels [29]. These gels exhibit interesting lithium redox intercalation properties but their electrochemical behavior has not
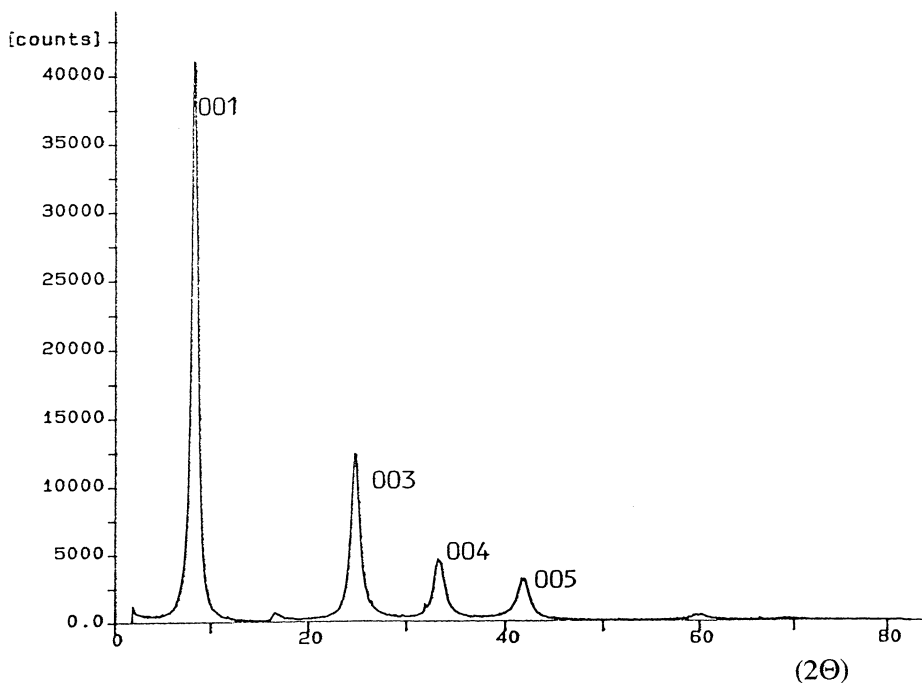
Fig. 6. X-ray diffraction pattern of a film of $V_2O_5 \cdot 1.8H_2O$ xerogel in transmission geometry.

been reported. Adding a small amount of PEO to the gel prior to casting improves significantly the mechanical properties of the film for the realization of micro-batteries [21].

4.4. Electrochemical properties of vanadium oxide gels

Vanadium pentoxide xerogels, $V_2O_5 \cdot nH_2O$ exhibit both ionic and electronic conduction. This is due to the partial reduction of V^{5+} into V^{4+} and the acid behavior of OH groups. Their electrical conductivity increases as the amount of V^{4+} increases ($\sigma_{300} \approx 4 \times 10^{-5}$ Ω^{-1} cm^{-1} for $V^{4+} = 1\%$, $\sigma_{300} \approx 2 \times 10^{-3}$ Ω^{-1} cm^{-1} for $V^{4+} = 10\%$). Anti static coatings based on vanadium pentoxide gels have then been patented by Kodak [22]. They also exhibit fast proton conduction and the a.c. conductivity of thin films increases with the water content, i.e. with the water pressure ($\sigma_{300} \approx 3 \times 10^{-2}$ Ω^{-1} cm^{-1} for $n + 1.6$, $\sigma_{300} \approx 5 \times 10^{-5}$ Ω^{-1} cm^{-1} for $n + 0.5$). Humidity sensors have been developed taking advantage of this property [23]. They are made of V_2O_5 gels mixed with an organic polymer (hydroxy propyl methyl cellulose). The impedance of these hybrid films decreases by about two orders of magnitude when the relative humidity increases from 80 to 97%.

Vanadium oxide xerogels have been extensively studied as reversible cathodes for lithium batteries [9]. Chemical bonds between V_2O_5 ribbons in vanadium oxide

xerogels are much weaker than in the crystalline oxide. Water molecules are intercalated in the interlamellar space and ionic species can diffuse easily through the materials. The electrochemical behavior of vanadium pentoxide gels $V_2O_5 \cdot nH_2O$ as a reversible cathode for lithium batteries is therefore quite different from that of the crystalline oxide. Moreover, thin layers can be easily deposited onto various substrates allowing the fabrication of micro-batteries.

The discharge curve of vanadium pentoxide xerogels exhibits a single plateau around 3.1 V (Fig. 7). A faradaic yield close to 1.8 e/V_2O_5 and a capacity of 250 Ah kg^{-1} are obtained at 2 V corresponding to the reduction of all V^{5+} ions into V^{4+} [24]. Cycling experiments show a good reversibility and almost 70% of the initial capacity is recovered after 30 cycles for a current density $j = 0.05$ mA cm^{-2} [25].

The intercalation of metal ions such as Na$^+$ within the layered structure of vanadium pentoxide gels has been used for the low temperature synthesis of vanadium bronzes. The ordered stacking of the ribbons is preserved during a thermal treatment leading to the crystallization around 350°C of anisotropic films of vanadium bronzes [26]. These sol-gel bronzes exhibit the same structure as the usual β-Na$_x$V$_2$O$_5$ vanadium bronzes obtained via solid state reactions at 700°C. However, X-ray diffraction suggests that (a,c) planes are preferentially oriented parallel to the substrate, while the tunnels of the bronze structure remain perpendicular to the substrate.

This orientation of sol-gel layers enhances the diffusion of Li$^+$ ions into the host lattice and sol-gel bronzes exhibit improved electrochemical properties. The
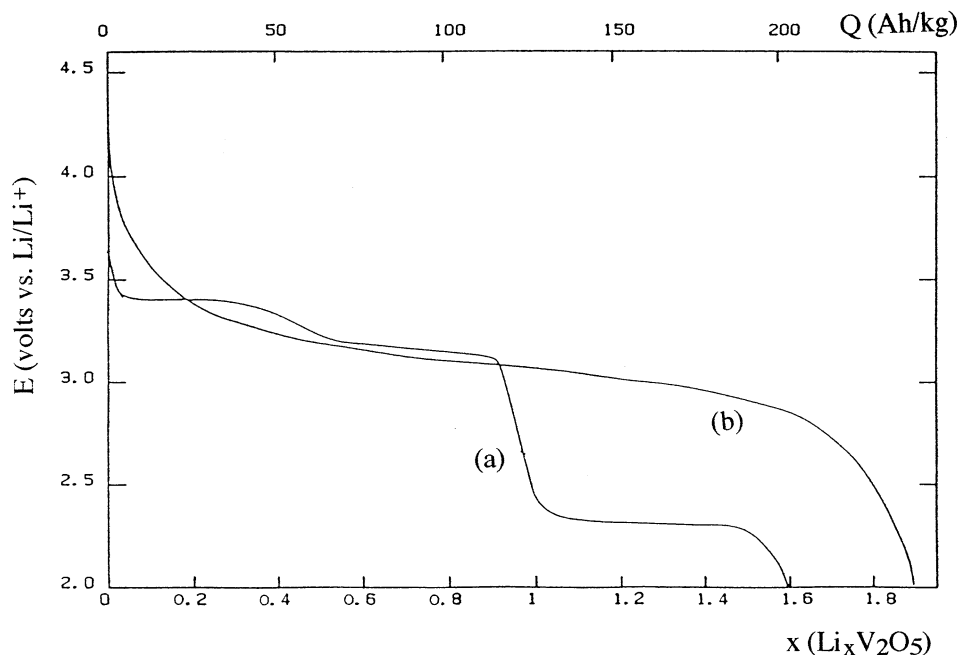

Fig. 7. Discharge curve of (a) crystalline V_2O_5; (b) vanadium oxide xerogel.

faradaic yield of β-$Na_xV_2O_5$ is about twice larger than for the corresponding solid state bronzes. The chemical diffusion coefficient of lithium ($D_{Li} \approx 10^{-10}$ cm^2 s^{-1} for $0 < x < 0.3$) is almost two orders of magnitude larger than in the solid state derived bronze. The reversibility remains good in the potential range 3.8–1.8 V. A capacity of about 120 Ah kg^{-1} is still recovered after 50 cycles, twice the capacity obtained for solid state bronzes [27,28].

New crystalline phases such as $Fe_{0.12}V_2O_{5.16}$ have been synthesized via the intercalation of Fe^{3+} ions into the layered structure of vanadium pentoxide gels [29]. The presence of Fe^{3+} ions in the vanadium pentoxide matrix provides improved cycling properties at high discharge–charge rates (C/4). A specific capacity of 200 Ah kg^{-1} is recovered after 40 cycles in the 3.8–2 V potential range.

5. Conclusion

Sol-gel chemistry provides a very versatile route for the synthesis of oxide materials. This paper shows that a large variety of materials can be obtained from a single alkoxide precursor $VO(OR)_3$. VO_2 thin films can be easily deposited from alkoxide solutions. They exhibit a highly reversible metal-insulating transition and could be used as optical power limiting devices against laser aggression. Some partial hydrolysis occurs when the alkoxide film is left in air. An amorphous oxo-polymer is then formed that exhibit electronic conductivity and electrochromic properties. Layered vanadium oxide gels $V_2O_5 \cdot nH_2O$ are obtained in the presence of an excess of water. The ribbon-like structure of the oxide particles leads to the formation of fluid mesophases and oriented xerogel films.

Acknowledgements

References

[1] C.J. Brinker, G.W. Scherer, Sol-Gel Science, Academic Press, San Diego, 1990.
[2] J. Livage, M. Henry, C. Sanchez, Progr. Solid State Chem. 18 (1988) 259.
[3] L. Klein (Ed.), Sol-Gel Technology, Noyes, Park Ridge, USA, 1988.
[4] J. Livage, Chem. Mater. 3 (1991) 578.
[5] G. Guzman, R. Morineau, J. Livage, Mater. Res. Bull. 29 (1994) 509.
[6] Z.A.E.P. Vroon, C.I.M.A. Spee, J. Non-Cryst. Solids 218 (1997) 189.
[7] G. Guzman, F. Beteille, R. Morineau, J. Livage, J. Mater. Chem. 6 (1996) 505.
[8] J. Livage, Solid State Ion. 50 (1992) 307.
[9] J. Livage, Solid State Ion. 86 (1996) 935.
[10] N.T. Be Bay, P.M. Tien, S. Badilescu, Y. Djaoued, G. Bader, F.E. Girouard, V. Truong, L.Q. Nguyen, J. Appl. Phys. 80 (1996) 7041.
[11] J.J. Legendre, J. Livage, J. Colloid Interface Sci. 94 (1983) 75.

[12] T. Yao, Y. Oka, N. Yamamoto, Mater. Res. Bull. 27 (1992) 669.
[13] P. Davidson, A. Garreau, J. Livage, Liq. Cryst. 16 (1994) 905.
[14] P. Davidson, P. Batail, J.C.P. Gabriel, J. Livage, C. Sanchez, C. Bourgaux, Prog. Polym. Sci. 22 (1997) 913.
[15] X. Commeinhes, P. Davidson, C. Bourgaux, J. Livage, Adv. Mater. 9 (1997) 900.
[16] P. Aldebert, N. Baffier, N. Gharbi, J. Livage, Mater. Res. Bull. 16 (1981) 669.
[17] P. Aldebert, N. Baffier, J.J. Legendre, J. Livage, Rev. Chim. Miner. 19 (1982) 485.
[18] M.G. Kanatzidis, C.G. Wu, H. Marcey, D.C. DeGroot, C.R. Kannewurf, Chem. Mater. 2 (1990) 222.
[19] Y.J. Liu, D.C. DeGroot, J.L. Schindler, C.R. Kannewurf, M.G. Kanatzidis, Chem. Mater. 3 (1991) 525.
[20] F. Leroux, B.E. Koene, L.F. Nazar, J. Electrochem. Soc. 143 (1996) L181.
[21] G.M. Kloster, J.A. Thomas, P.W. Brazis, C.R. Kannewurf, D.F. Shriver, Chem. Mater. 8 (1996) 2418.
[22] C. Guestaux, J. Leauté, C. Virey, J. Vial, Patent No 3 658 573 (1972).
[23] A. Inubushi, S. Masuda, M. Okubo, A. Matsumoto, H. Sadamura, K. Suzuki, in: P. Vicenzini (Ed.), High Tech Ceramics, Elsevier, Amsterdam, 1987, p. 2165.
[24] J.P. Pereira-Ramos, L. Znaidi, N. Baffier, R. Messina, Solid State Ion. 28 (1988) 886.
[25] S. Bach, J.P. Pereira-Ramos, N. Baffier, R. Messina, J. Electrochem. Soc. 137 (1990) 1042.
[26] L. Znaidi, N. Baffier, M. Huber, Mater. Res. Bull. 24 (1989) 1501.
[27] R. Baddour, J.P. Pereira-Ramos, R. Messina, J. Perichon, J. Electroanal. Chem. 277 (1990) 359.
[28] R. Baddour, J.P. Pereira-Ramos, R. Messina, J. Perichon, J. Electroanal. Chem. 314 (1991) 81.
[29] S. Maingot, R. Baddour, J.P. Pereira-Ramos, N. Baffier, P. Wilman, J. Electrochem. 11 (1993) L158.